

Redistribution of Ca^{2+} among cytosol and organelle during stimulation of bovine chromaffin cells

CARLOS VILLALOBOS, LUCÍA NUÑEZ, MAYTE MONTERO, ANTONIO G. GARCÍA,*
MARIA TERESA ALONSO, PABLO CHAMERO, JAVIER ALVAREZ,
AND JAVIER GARCÍA-SANCHO¹

Instituto de Biología y Genética Molecular (IBGM), Universidad de Valladolid y Consejo Superior de Investigaciones Científicas, Departamento de Fisiología y Bioquímica, Facultad de Medicina, E-47005 Valladolid, Spain; and *Instituto Teófilo Hernando, Departamento de Farmacología y Terapéutica, Facultad de Medicina, Universidad Autónoma de Madrid, E-28029 Madrid, Spain.

ABSTRACT Recent results indicate that Ca^{2+} transport by organelle contributes to shaping Ca^{2+} signals and exocytosis in adrenal chromaffin cells. Therefore, accurate measurements of $[\text{Ca}^{2+}]$ inside cytoplasmic organelle are essential for a comprehensive analysis of the Ca^{2+} redistribution that follows cell stimulation. Here we have studied changes in Ca^{2+} inside the endoplasmic reticulum, mitochondria, and nucleus by imaging aequorins targeted to these compartments in cells stimulated by brief depolarizing pulses with high K^+ solutions. We find that Ca^{2+} entry through voltage-gated Ca^{2+} channels generates subplasmalemmal high $[\text{Ca}^{2+}]_c$ domains adequate for triggering exocytosis. A smaller increase of $[\text{Ca}^{2+}]_c$ is produced in the cell core, which is adequate for recruitment of the reserve pool of secretory vesicles to the plasma membrane. Most of the Ca^{2+} load is taken up by a mitochondrial pool, M1, closer to the plasma membrane; the increase of $[\text{Ca}^{2+}]_M$ stimulates respiration in these mitochondria, providing local support for the exocytotic process. Relaxation of the $[\text{Ca}^{2+}]_c$ transient is due to Ca^{2+} extrusion through the plasma membrane. At this stage, mitochondria release Ca^{2+} to the cytosol through the $\text{Na}^+/\text{Ca}^{2+}$ exchanger, thus maintaining $[\text{Ca}^{2+}]_c$ discretely increased, especially at core regions of the cell, for periods that outlast the duration of the stimulus.—Villalobos, C., Nuñez, L., Montero, M., García, A. G., Alonso, M. T., Chamero, P., Alvarez, J., García-Sancho, J. Redistribution of Ca^{2+} among cytosol and organelle during stimulation of bovine chromaffin cells. *FASEB J.* 16, 343–353 (2002)

Key Words: calcium · mitochondria · aequorin · nucleus

CELL STIMULATION IS often associated with an increase of the cytosolic Ca^{2+} concentration ($[\text{Ca}^{2+}]_c$) that transduces the appropriate cellular responses. In chromaffin cells, Ca^{2+} entry through voltage-operated Ca^{2+} channels (VOCC) of the plasma membrane is essential for triggering the secretory response (1). Since Ca^{2+} may act on many different effectors at different subcellular locations, considerable attention has been paid to

the spatiotemporal profiles of $[\text{Ca}^{2+}]_c$ transients. Diffusion of Ca^{2+} through the cytosol, cytosolic Ca^{2+} buffering, and Ca^{2+} transport by organelle are essential for shaping the $[\text{Ca}^{2+}]_c$ transients. Changes of $[\text{Ca}^{2+}]$ inside organelle may also be relevant to determine cell responses (2–4).

Cytosolic Ca^{2+} buffering and diffusion in bovine chromaffin cells have been studied by Neher and co-workers (5, 6). The cytosol has a total binding capacity of 4 mM and the endogenous Ca^{2+} buffer is poorly mobile, fast (association rate = $10^{-8} \text{ M}^{-1}\text{s}^{-1}$), and with low affinity for Ca^{2+} (dissociation constant = 100 μM). The activity coefficient of the endogenous buffer is $\sim 1/40$. Cytosolic buffering slows down Ca^{2+} mobility to reach an apparent diffusion of $\sim 10^{-7} \text{ cm}^2\text{s}^{-1}$. The 2-dimensional apparent diffusion coefficient is $\sim 40 \mu\text{m}^2/\text{s}$ and shows inhomogeneities at the nuclear envelope and at the plasma membrane (7). Brief opening of VOCC generates microdomains of high $[\text{Ca}^{2+}]_c$ near the mouth of the channel that can be detected in Ca^{2+} imaging measurements (8). In such microdomains, Ca^{2+} can reach concentrations as high as 10 μM and perhaps 100 μM (2, 9). Because of rapid diffusion of Ca^{2+} toward the surrounding cytosol, $[\text{Ca}^{2+}]_c$ microdomains are highly restricted in time and space (2, 10).

The Ca^{2+} fluxes relevant to determine $[\text{Ca}^{2+}]_c$ transients after stimulation of chromaffin cells are entry and extrusion at the plasma membrane and uptake and release at the cytoplasmic organelle. Among the last, the endoplasmic reticulum (ER) and mitochondria seem to be the most directly involved. Secretory granules contain large amounts of calcium, but exchange through their membrane is too slow to contribute to $[\text{Ca}^{2+}]_c$ transients (but see ref 11).

Ca^{2+} entry through VOCC and its subsequent clearance have been studied extensively in bovine and rat chromaffin cells (5, 6, 12, 13). Membrane depolarization to 0 mV elicits Ca^{2+} currents peaking near 800 pA

¹ Correspondence: IBGM, Departamento de Fisiología y Bioquímica, Facultad de Medicina, E-47005 Valladolid, Spain. E-mail: jgsancho@ibgm.uva.es

and deactivating with half-time constants of 300–500 ms. In bovine chromaffin cells, a 0.5 s stimulation period typically elicits a mean I_{Ca} of 250 pA. In terms of Ca^{2+} flow, this current is equivalent (for a 15 μ m diameter cell) to 700 μ mol/l of cells/s (5). Measurements of ^{45}Ca uptake by bovine chromaffin cells depolarized with high K^+ (59 mM) was linear during the first 5 s at an estimated rate of $0.7 \cdot 10^{-15}$ mol per cell/s, which is equivalent to 400 μ mol/l of cells/s (14).

Plasma membrane Ca^{2+} extrusion is due to operation of a plasma membrane Ca^{2+} ATPase and an Na^+/Ca^{2+} exchange system. The joint action of both transport systems has been estimated to decrease $[Ca^{2+}]_c$ at a maximal rate of ~ 0.2 μ M/s, equivalent to 20 μ mol/l cells/s, in rat chromaffin cells at 27°C (12, 13).

Most of the information on transport parameters by organelle in intact cells is indirect, inferred from their effects on $[Ca^{2+}]_c$. Maximal uptake by ER is considered to contribute little, perhaps 1–1.5 μ M/s (equivalent to 40–60 μ mol/l cells/s), to changes in $[Ca^{2+}]_c$ during stimulation of bovine (6) and rat (13) chromaffin cells. It has been shown recently that cytosolic Ca^{2+} may trigger Ca^{2+} -induced Ca^{2+} release (CICR) from the ER of bovine chromaffin cells (15).

Ca^{2+} transport by mitochondria has received renewed attention in the last few years, both because of possible participation in shaping $[Ca^{2+}]_c$ transients and because changes of intramitochondrial $[Ca^{2+}]$ ($[Ca^{2+}]_M$) seem important by themselves for the regulation of cell functions, such as the rate of respiration or programmed cell death (16, 17). Ca^{2+} is taken up through the Ca^{2+} uniporter, a low-affinity/high-capacity system driven by the mitochondrial membrane potential (18). Ca^{2+} exit from mitochondria through an Na^+/Ca^{2+} exchanger and through an Na^+ -independent system, the first being dominant in the adrenal gland (18, 19). The activity coefficient of Ca^{2+} inside the mitochondrial matrix seems to be very low, in the 1/1000 range (20–22). It has been shown that mitochondria can contribute to clearing cytosolic Ca^{2+} loads in rat (13, 21) and cow (6) chromaffin cells. Herrington et al. (13) reported mitochondrial uptake rates of (in terms of changes of $[Ca^{2+}]_c$) 0.4 to 0.7 μ M/s at $[Ca^{2+}]_c$ concentrations of 0.5–2 μ M. Xu et al. (6) report much larger rates: 120 μ M/s at saturating $[Ca^{2+}]_c$ concentrations (200 μ M). These differences are consistent with the $[Ca^{2+}]_c$ dependence of the activity of the mitochondrial Ca^{2+} uniporter (23, 24).

We have recently shown the validity of using targeted aequorins with different Ca^{2+} affinities to monitor directly changes of $[Ca^{2+}]$ inside ER and mitochondria of living chromaffin cells (15, 23–25). Taking advantage of this technology, we attempt here a quantitative explanation of fluxes among the extracellular, cytosolic, and organellar compartments during depolarization of chromaffin cells leading to Ca^{2+} entry through VOCC.

MATERIALS AND METHODS

Cell culture, $[Ca^{2+}]_c$ measurements, and expression of aequorins

Isolation and culture of bovine adrenal chromaffin cells was as described (15). Cells were plated on 12 mm glass poly-D-lysine-coated coverslips ($1\text{--}5 \times 10^5$ cells; 0.5 ml) and maintained at 37°C in a humidified atmosphere of 5% CO_2 . $[Ca^{2+}]_c$ imaging in cells loaded with either Fura-2 (26) or fura-4F (24) was as described previously. Recombinant aequorins containing targeting sequences to several subcellular locations (27) have been used. Both wild-type aequorin and mutated (Asp119→Ala), low Ca^{2+} affinity aequorin (AEQmut; ref 28) were used. For aequorin expression, cells were infected with a defective herpes simplex virus type 1 (HSV-1) containing the corresponding chimeric aequorin gene and cultured for 12–24 h prior to measurement. Viruses expressing mitochondrial aequorin (mitAEQ), low Ca^{2+} affinity mutated mitochondrial (mitAEQmut), or ER (erAEQmut) aequorins have been described (15, 23, 24). Nuclear (nucleoplasmic) and cytosolic aequorin cDNAs were obtained from Molecular Probes (Eugene, OR) and cloned in the pHSVpUC plasmid. Packaging and titration of the pHSVnucAEQ (nuclear) and pHSVcytAEQ (cytosolic) viruses were performed as reported before (25). The multiplicity of infection was from 0.01 to 0.1 for batch luminescence measurements (15, 24) and from 0.3 to 1 for bioluminescence imaging.

Measurements of aequorin bioluminescence and NAD(P)H fluorescence

Cells expressing apoaequorins were incubated for 1–2 h at room temperature with 1 μ M coelenterazine. Coelenterazine n was used to reconstitute mitAEQmut in order to decrease further Ca^{2+} affinity (29). Batch cell aequorin photoluminescence measurements were performed as described (15, 24) and calibrations in $[Ca^{2+}]_c$ were done using published constant values (30). For bioluminescence imaging (31, 32), cells were placed into a perfusion chamber thermostated to 37°C under a Zeiss Axiovert S100 TV microscope (objective, Fluor 40 \times oil, 1.3 n.a.) and perfused at 5–10 ml/min with test solutions prewarmed at 37°C. The standard incubation medium had the following composition (in mM): NaCl, 145; KCl, 5; $CaCl_2$, 1; $MgCl_2$, 1; glucose, 10; sodium-HEPES, 10, pH 7.4. At the end of each experiment, cells were permeabilized with 0.1 mM digitonin in 10 mM $CaCl_2$ to release all residual aequorin counts. Images were taken with a Hamamatsu VIM photon-counting camera handled with an Argus-20 image processor and integrated for 10 s periods. Photons/cell in each image were quantified using the Hamamatsu Aquacosmos software. Total counts per cell ranged between $3 \cdot 10^3$ and $3 \cdot 10^5$ and noise was (mean \pm SD) 1 ± 1 c.p.s. per typical cell area (3000 pixels). Values are referred to the whole cell area. Data were first quantified as rates of photoluminescence emission/total c.p.s remaining at each time and divided by the integration period (L/L_{TOTAL} in s^{-1}). Calibrations in $[Ca^{2+}]_c$ were performed using published constant values (30). A transmission image was also taken at the beginning of each experiment.

Mitochondrial NAD(P)H fluorescence was measured using the same set up as for aequorin with excitation at 340 ± 10 nm and emission at 450 ± 40 nm. The integration period was 6 s. For these experiments, 1 mM pyruvate was added to the standard medium in order to keep the cytosolic NAD in the oxidized state.

Coelenterazines and the acetoxymethyl (AM) esters of fura-2 and fura-4F were obtained from Molecular Probes.

CGP37157 was from Tocris (Bristol, UK). Other reagents were of the highest quality available from Sigma (St. Louis, MO) Calbiochem (San Diego, CA), or Merck (Rahway, NJ).

RESULTS

Increase of $[Ca^{2+}]_c$ upon stimulation with high K solutions

To induce Ca^{2+} entry through VOCC, cells were depolarized by stimulation with high K^+ (75 mM) solution for 10 s. Experiments in cells loaded with fura-2 showed quite a homogeneous response, with estimated average $[Ca^{2+}]_c$ peaks of 1.7–2 μM . There was, however, a clear tendency to saturation of the dye in many cells (not shown); this would lead to an underestimation of the $[Ca^{2+}]_c$ concentrations. To circumvent this problem, fura-4F, which has a smaller affinity for Ca^{2+} ($K_d=0.77 \mu M$), was used. **Figure 1** illustrates a typical experiment in which the cells were stimulated by two consecutive high K^+ pulses. The peak $[Ca^{2+}]_c$ reached 4.8 μM in this experiment (Fig. 1A). In five similar experiments, the average $[Ca^{2+}]_c$ peak (expressed as $\Delta[Ca^{2+}]_c$; mean \pm SD; $n=213$ cells) was $4.05 \pm 1.41 \mu M$. The rates of $[Ca^{2+}]_c$ change are shown in Fig. 1B. The increase of $[Ca^{2+}]_c$ reached a maximum rate of $\sim 1.1 \mu M/s$ during stimulation. In five similar experiments, the average value was (mean \pm SD) $1.15 \pm 0.15 \mu M/s$. In two similar

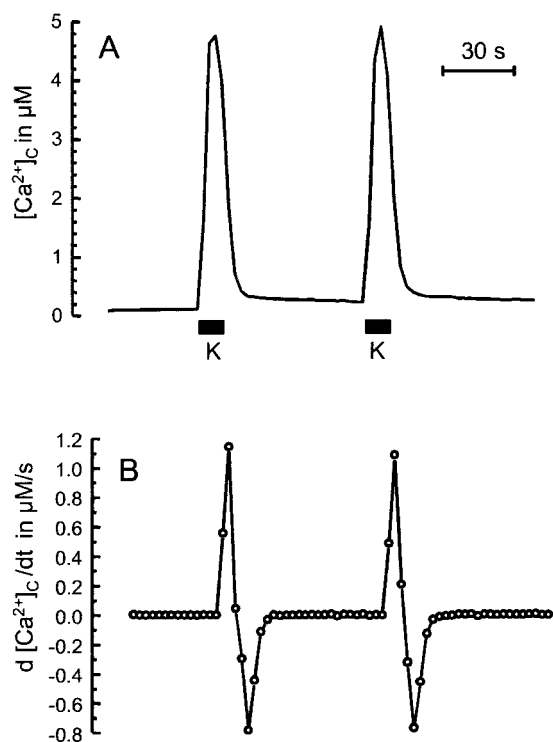


Figure 1. Increase of $[Ca^{2+}]_c$ in response to repeated stimulation with high K^+ solution. Measurements performed at $37^\circ C$ in cells loaded with fura-4F; time resolution, 2.5 s. K, 75 mM KCl. A) Time course of the $[Ca^{2+}]_c$ changes; average of 58 single cells. B) Instantaneous rates of $[Ca^{2+}]_c$ changes; same cells as in panel A.

experiments performed at $22^\circ C$, changes of $[Ca^{2+}]_c$ were similar in both peak amplitude (mean \pm SD, $4.05 \pm 1.51 \mu M$; $n=75$) and kinetics (the maximum rate of $[Ca^{2+}]_c$ increase ranged between 0.7 and 1 $\mu M/s$ in four independent measurements; results not shown).

The rate of $[Ca^{2+}]_c$ increase measured here is much smaller than expected from typical I_{Ca} or ^{45}Ca uptake measurements. For an activity coefficient of 1/40 for the cytosolic Ca^{2+} buffers (5, 6), Ca^{2+} entry would be expected to increase $[Ca^{2+}]_c$ at a rate of 10–17.5 $\mu M/s$, which is one order of magnitude larger than measured in cells loaded with fura-4F. These results suggest that most Ca^{2+} entering the cell during the 10 s stimulation period is taken up into organelle.

Once the stimulation pulse ends, Ca^{2+} is cleared from the cytosol at a rate of $\sim 0.7 \mu M/s$, which declines quickly as $[Ca^{2+}]_c$ approaches its prestimulation value (Fig. 1B). At this stage, Ca^{2+} clearance (unopposed by Ca^{2+} entry) reflects the joint action of uptake into organelle and extrusion through the plasma membrane.

Uptake of Ca^{2+} by the ER

The uptake of Ca^{2+} by the ER can be monitored precisely using targeted aequorins with low Ca^{2+} affinity (15, 25, 29, 33). **Figure 2A** shows the time course of ER refilling in Ca^{2+} -depleted chromaffin cells upon incubation with Ca^{2+} -containing medium, measured at $22^\circ C$. On addition of Ca^{2+} , $[Ca^{2+}]_{ER}$ increased to 500–600 μM in 2–3 min. The maximum rate of the $[Ca^{2+}]_{ER}$ increase was $\sim 5.5 \mu M/s$. In 12 similar experiments, the maximum rate was (mean \pm SD) 4.5 ± 1.3 . This value decreased to 0.8 $\mu M/s$ in cells loaded with BAPTA and increased to 9.0 ± 3.2 ($n=8$) when cells were depolarized with high K^+ solution during the refilling period (data not shown). At $37^\circ C$, uptake is \sim fourfold faster (33), which gives a maximum figure of $\sim 36 \mu M/s$. Assuming an activity coefficient of 1/20 and a volume of 10% relative to the cytosol (3, 34), this value would be equivalent to 72 $\mu mol/l$ cells/s, which is still one order of magnitude smaller than the value estimated for Ca^{2+} influx through VOCC. When Ca^{2+} influx takes place in cells with Ca^{2+} -filled ER, net Ca^{2+} release rather than Ca^{2+} uptake is produced (Fig. 2B), an expression of the activation of the CICR mechanism (15). We conclude that the ER could not be responsible of the buffering of $[Ca^{2+}]_c$ during stimulation of bovine chromaffin cells. Based on measurements of $[Ca^{2+}]_c$ clearance and the effects of inhibitors of SERCA ATPases, Neher and co-workers (6) and Hille and co-workers (13) arrived to the same conclusion in bovine and murine chromaffin cells, respectively.

Uptake of Ca^{2+} by mitochondria and nucleus

We have shown before that the bovine chromaffin cell mitochondria accumulate large amounts of Ca^{2+} during stimulation with either high K^+ solutions, acetylcholine, or caffeine (23). The Ca^{2+} load was taken up selectively into a mitochondrial pool amounting to 50%

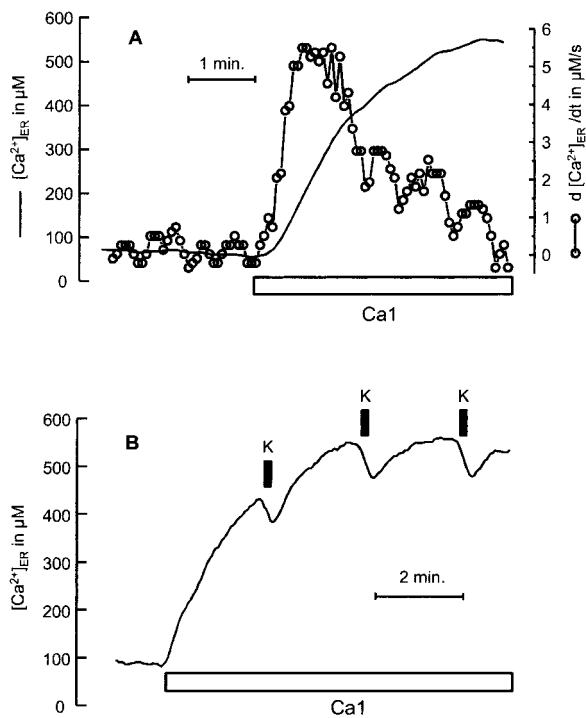


Figure 2. Ca^{2+} uptake by the ER. All measurements were performed in cells expressing mutAEQer reconstituted with coelenterazine n at 22°C. Cell batch measurements. Cells suspended in Ca^{2+} -free medium. CaCl_2 (1 mM) added as shown. *A*) Time course of the $[\text{Ca}^{2+}]_{\text{ER}}$ changes (continuous line) and instantaneous rates of uptake (circles). *B*) Effects of high K^+ pulses (K, 75 mM KCl).

of the total (pool M1); the other half (pool M2) takes up much smaller amounts (23). A similar conclusion was reached by Pivovarova et al. (35) for rat chromaffin cells by studying mitochondrial calcium content by electron microscopy X-ray microanalysis.

Figure 3A shows new measurements performed at the single cell level. Cells expressing the mitochondria-targeted aequorin were repeatedly stimulated with high K^+ solution or caffeine and then permeabilized with digitonin to burn up the remaining aequorin. Representative images corresponding to each pulse are shown at the top; photoluminescence emission (expressed as L/L_{TOTAL} , s^{-1} ; see Materials and Methods) and aequorin consumption by one of the cells are shown below. About 40% of the aequorin was consumed during the first stimulus, but subsequent stimuli had a much smaller effect. Permeabilization with digitonin burned up the remaining half of the aequorin pool. This contrasts with the changes in $[\text{Ca}^{2+}]_{\text{c}}$ accomplished by repeated stimulation with high K^+ , which were reproducible (Fig. 1A; see also ref 23). We performed another series of experiments using nucleus-targeted aequorin (Fig. 3B). Here the behavior was the same as that found for $[\text{Ca}^{2+}]_{\text{c}}$: each stimulus produced similar aequorin consumption (~5% of the total) and luminescence emission. Similar results were reported for the cytosolic aequorin (not shown).

Figure 4A shows the average consumption of the mitochondria-targeted aequorin ($\pm\text{SE}$) of 55 cells present in

the same microscope field together with the responses of four individual cells selected to illustrate the range of variation observed. Even though there were differences among the extent of the responses of individual cells, in all cases the response to the second stimulus was much smaller than to the first one. Figure 4B shows calibrated $[\text{Ca}^{2+}]_{\text{M}}$ responses for the same experiment. The first Ca^{2+} peak reached ~10 μM ; the ensuing ones consistently reached only 2–4 μM . Using aequorin reconsti-

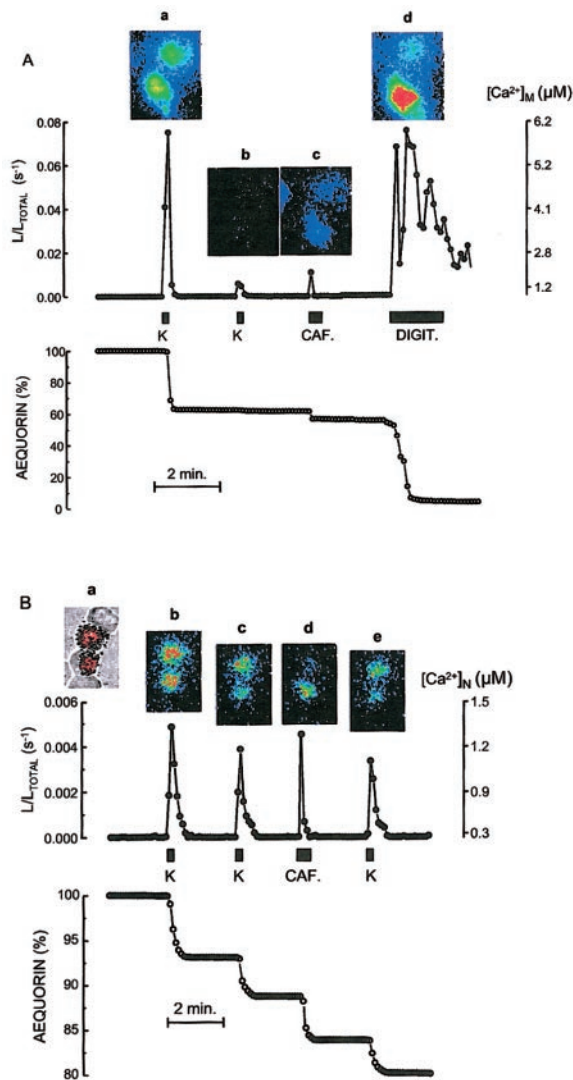


Figure 3. Effects of repeated stimulation with high K^+ on $[\text{Ca}^{2+}]_{\text{M}}$ and $[\text{Ca}^{2+}]_{\text{N}}$. *A*) Photoluminescence imaging of cells expressing mitAEQ. Experiments performed at 37°C. Time resolution, 10 s. The upper trace shows the changes of luminescence in a representative single cell. Calibration scale in $[\text{Ca}^{2+}]_{\text{M}}$ is shown at right. Images of two single cells taken during $[\text{Ca}^{2+}]_{\text{M}}$ peaks are also shown. Luminescence is coded in pseudocolor, from dark blue to red. K, 75 mM KCl; CAF, 50 mM caffeine. DIGIT, 0.1 mM digitonin + 10 mM Ca^{2+} . The traces correspond to the cell at bottom. The lower trace shows cumulative aequorin consumption (% remaining in the cell) in the same cell. *B*) Photoluminescence imaging of cells expressing nucAEQ. In image *a*, integrated luminescence (in red) has been superimposed to the gray transmission image to show restricted location of aequorin. Other details as in panel *A*.

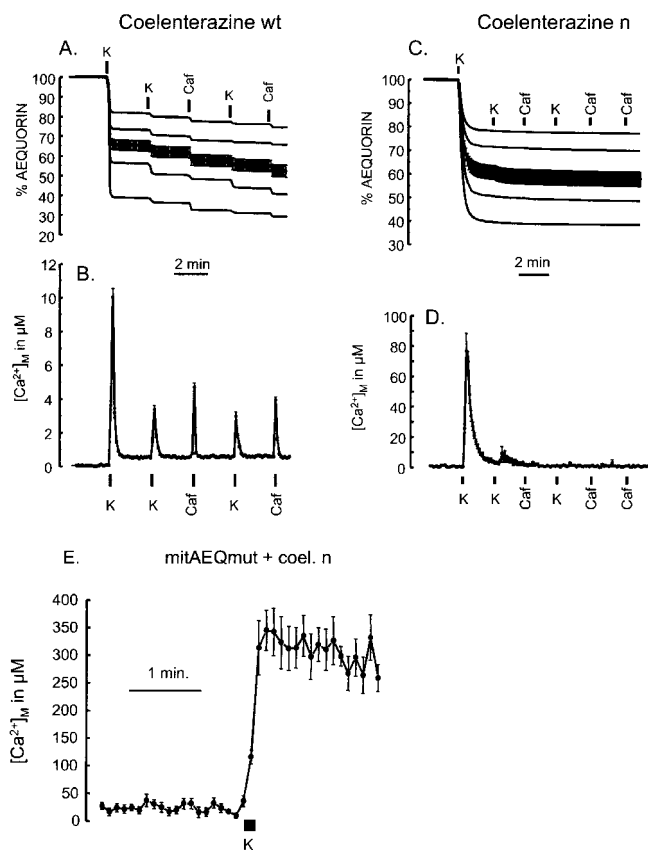


Figure 4. Effects of repeated stimulation with high K^+ on $[Ca^{2+}]_M$. Photoluminescence imaging was performed in cells expressing mitAEQ reconstituted with either wild-type coelenterazine (measuring range 0.3–10 μM ; A, B) or coelenterazine n (measuring range 1–100 μM ; C, D). Temperature, 22°C. Other details as in Fig. 3. Circles represent the mean \pm SE of 38 (A) and 21 (B) single cells. Lines without symbols in panels A, C represent four individual cells selected to illustrate the range of variation. E) Photoluminescence imaging was performed at 22°C in cells expressing mitAEQmut reconstituted coelenterazine n (measuring range 50–1000 μM). Values are mean \pm SE of 10 single cells.

tuted with coelenterazine n, which has a lower affinity for Ca^{2+} (measuring range 1–100 μM , ref 23), behavior regarding aequorin consumption was similar (Fig. 4C). The calibrated signal (Fig. 4D) now revealed a $[Ca^{2+}]_M$ peak of ~ 80 μM for the first stimulus; the second reached only 8 μM and subsequent ones were in the 2–4 μM range, which is barely detectable for this aequorin–coelenterazine combination.

We conclude from the above experiments that Ca^{2+} is taken up during the first stimulus into a fraction of mitochondria (pool M1, amounting to $\sim 50\%$ of the total mitochondrial pool) at a high enough concentration to burn out all its aequorin. Because of this, the ensuing high K^+ stimuli do not produce light emission from this pool. The other half of the mitochondria (pool M2) takes up much smaller amounts of Ca^{2+} , resulting in a modest light emission that is seen uncontaminated during the last stimuli. The aequorin contained into pool M2, however, is burned out upon permeabilization with digitonin (Fig. 3A).

The extent of the uptake of Ca^{2+} into pool M1 can be quantified using a mutated, low Ca^{2+} affinity aequorin reconstituted with coelenterazine n (mitAEQmut) that can report Ca^{2+} concentrations as high as 10^{-3} M for several minutes (23). Due to its lower Ca^{2+} affinity, this aequorin is burned only partly during each stimulation with high K^+ . Figure 4E shows the average response (\pm SE) of 10 single cells to a challenge with high K^+ , as reported by mitAEQmut reconstituted with coelenterazine n. $[Ca^{2+}]_M$ reached a peak of ~ 350 μM within 10–15 s, then decreased slowly (the decrease of $[Ca^{2+}]_M$ is especially slow because it was performed at 20°C, see below), remaining above 300 μM for at least 1 min. According to our estimates (see Materials and Methods), $> 90\%$ of the wild-type aequorin should be consumed by < 1 s when reconstituted with normal coelenterazine and within 1 min when reconstituted with coelenterazine n.

Figure 5A shows the time course of Ca^{2+} uptake, measured with mitAEQmut at 37°C, by the mitochondria of pool M1 during repeated stimulation with high K^+ solution. $[Ca^{2+}]_M$ increased to 300–400 μM by the end of the stimulation period. The rate of uptake reached maximum values of 40–50 $\mu\text{M}/\text{s}$ (Fig. 5B). In 18 similar measurements, the maximum rate of $[Ca^{2+}]_M$ increase was (mean \pm SD) 56 ± 12 $\mu\text{M}/\text{s}$. Assuming an activity coefficient of 1/1000 and a relative mitochondrial volume of 4%, this Ca^{2+} load would be equivalent to 1100 $\mu\text{mol}/\text{l}$ cells/s (taking into account that only 50% of the mitochondria take up Ca^{2+}). This value is similar to the one estimated for Ca^{2+} influx through VOCC, suggesting that most of the Ca^{2+} load taken up by the cell during stimulation can accumulate into mitochondria.

To study the kinetics of Ca^{2+} transport through the uniporter, we measured mitochondrial uptake in bovine chromaffin cells permeabilized by brief treatment with digitonin and perfused with different Ca^{2+} buffers (see Materials and Methods). Results are shown in Fig. 5C. The uptake was very slow at $[Ca^{2+}]_c$ below 2 μM , but increased steeply at higher concentrations. The line is the best fit to the equation:

$$v = \{V_{\max} \cdot ([Ca^{2+}]_c)^2 / \{ (K_{50})^2 + ([Ca^{2+}]_c)^2 \}}$$

for $V_{\max} = 158 \pm 7$ $\mu\text{M}/\text{s}$ and $K_{50} = 23 \pm 2$ μM . The K_{50} value is similar to both the one obtained earlier with isolated mitochondria from liver and heart and bovine adrenal medulla (10–15 μM ; refs 18, 19, 36) and the one estimated by Xu et al. (6) from measurements of the decrease of $[Ca^{2+}]_c$ in intact bovine chromaffin cells (40 μM). The value of V_{\max} would be equivalent to 6320 $\mu\text{mol}/\text{l}$ cells/s, not far from the 4800 value estimated by Xu et al. (6) at 200 μM $[Ca^{2+}]_c$.

Relaxation of $[Ca^{2+}]_c$ peaks

When Ca^{2+} entry through VOCC ceases, $[Ca^{2+}]_c$ begins to decrease as a result of multiple fluxes. Plasma membrane Ca^{2+} ATPase and Na^+/Ca^{2+} exchanger extrude Ca^{2+} from the cytosol to the extracellular

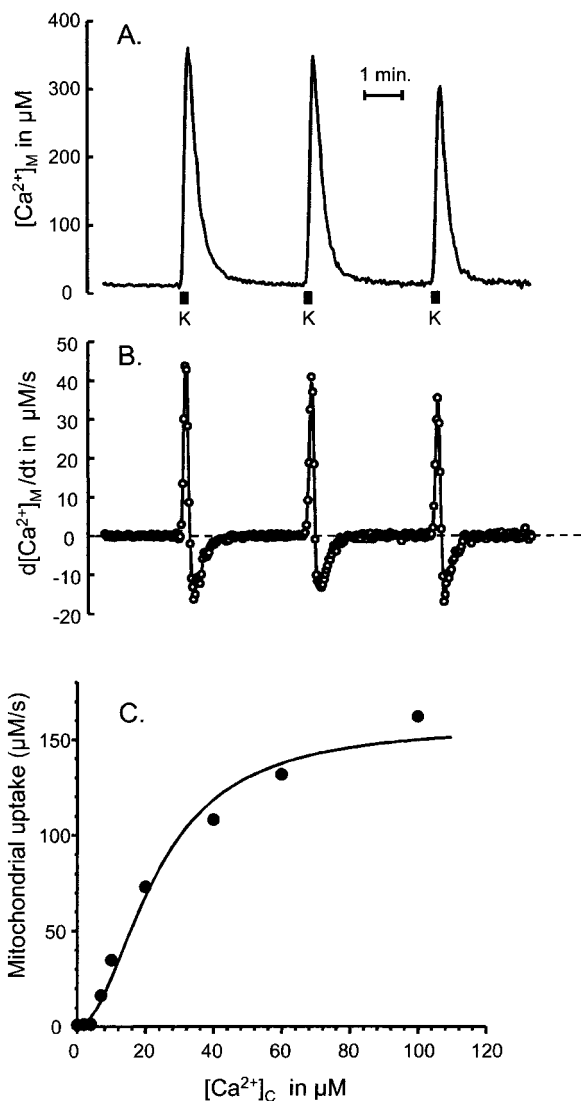


Figure 5. Time course and concentration dependence of mitochondrial Ca^{2+} uptake. Batch measurements performed in cells expressing mitAEQmut (reconstituted with coelenterazine n) at 37°C . Results have been corrected for a 50% of the mitochondrial pool (23). *A, B*) The time course and instantaneous rates of uptake in the same cells. *C*) Uptake in cells permeabilized with digitonin ($20\ \mu\text{M}$, 1 min) and incubated with HEDTA/ Ca^{2+} buffers at 37°C (23).

medium. We have not performed specific measurements of these fluxes, but an upper limit of $\sim 0.8\ \mu\text{M}/\text{s}$ can be estimated from the maximum rate of $[\text{Ca}^{2+}]_c$ decrease (Fig. 1C). The mean value from six independent measurements was (mean \pm SD) 0.73 ± 0.07 , which is equivalent to $29\ \mu\text{mol}/\text{l cells}/\text{s}$. Herrington et al. (13) have estimated a value of $\sim 0.3\ \mu\text{M}/\text{s}$ in rat chromaffin cells at 27°C . Assuming a Q_{10} value of 3–4, this value is comparable to our estimate.

If this maximum rate was sustained for a few seconds, the return of $[\text{Ca}^{2+}]_c$ to the prestimulation level would be extremely fast. However, the rate of $[\text{Ca}^{2+}]_c$ decline slows down quickly (Fig. 1C). Desaturation of the plasma membrane Ca^{2+} extrusion mechanism may help to slow down relaxation. However, the major

determinant of this $[\text{Ca}^{2+}]_c$ stabilization is that once it declines below $2\ \mu\text{M}$, plasma membrane Ca^{2+} extrusion is almost matched by Ca^{2+} release from the organella (see below).

Ca^{2+} release from the ER is comparatively quite slow. Upon treatment of chromaffin cells with cyclopiazonic acid, we find a maximal rate of $[\text{Ca}^{2+}]_{\text{ER}}$ decrease of $\sim 1.3\ \mu\text{M}/\text{s}$, which is equivalent to $2.6\ \mu\text{mol}/\text{l cells}/\text{s}$ (15). Release from mitochondria is much faster. Upon termination of the stimulus with high K^+ , $[\text{Ca}^{2+}]_M$ decreases at a maximal rate of $13\text{--}18\ \mu\text{M}/\text{s}$ (Fig. 5B). In five similar experiments, the maximum rate of $[\text{Ca}^{2+}]_M$ decrease was (mean \pm SD) $14.2 \pm 3.4\ \mu\text{M}/\text{s}$. Since exit takes place from only one-half of the mitochondrial pool, it would be equivalent to $280\ \mu\text{mol}/\text{l cells}/\text{s}$. This rate decreases quickly as $[\text{Ca}^{2+}]_M$ declines (Fig. 5B).

Kinetics of Ca^{2+} release from mitochondria loaded with Ca^{2+} is shown in Fig. 6. Traces A and B compare the time course of the $[\text{Ca}^{2+}]_M$ changes in control cells and in cells treated with CGP37157, an inhibitor of the mitochondrial $\text{Na}^+/\text{Ca}^{2+}$ exchanger. Traces C and D show the estimated rate constants and E a plot of exit against $[\text{Ca}^{2+}]_M$. As shown before (23, 24), CGP37157 slowed down Ca^{2+} efflux. In control cells, mitochondrial Ca^{2+} exit showed saturation at the higher $[\text{Ca}^{2+}]_M$ and a sigmoidal shape at the lower $[\text{Ca}^{2+}]_M$. In the presence of CGP37157, saturation and sigmoidicity both seemed to disappear (Fig. 6E). When we constructed a similar plot with the average results of 11 control experiments, the resulting data points could be well fitted by the following equation:

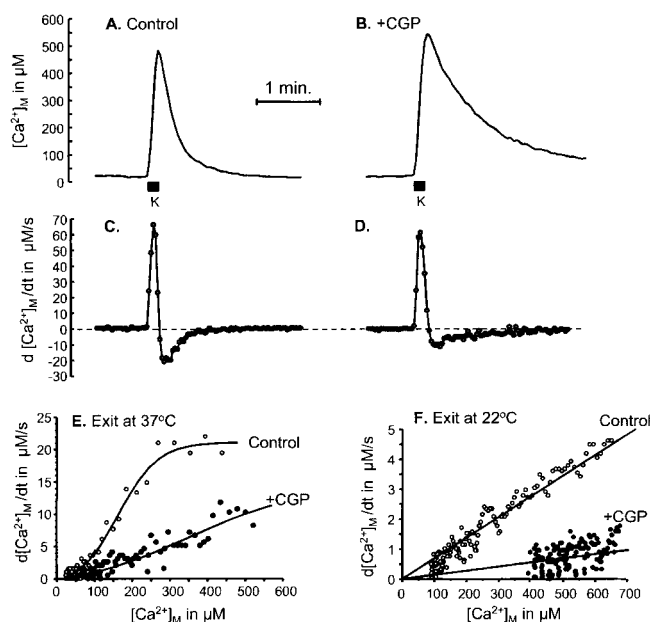


Figure 6. Exit of mitochondrial Ca^{2+} . The time course and instantaneous rates are compared in control cells (*A, C*) and cells treated with $20\ \mu\text{M}$ CGP37157 (*B, D*). Details as in Fig. 5. *E*) Concentration dependence of mitochondrial Ca^{2+} exit at 37°C ; the plot was constructed from data in panels A–D. *F*) Concentration dependence of mitochondrial exit at 22°C . Experiments performed with the same cell batch as in panel E.

$$v = \{V_{\max} \cdot ([Ca^{2+}]_M)^2\} / \{K_{50} + ([Ca^{2+}]_M)^2\}$$

with $K_{50} = 217 \pm 12 \mu\text{M}$ and $V_{\max} = 19.6 \pm 1.0 \mu\text{M/s}$. This V_{\max} value would be equivalent to $780 \mu\text{mol/l cells/s}$.

The efflux of Ca^{2+} from loaded mitochondria was also highly sensitive to temperature (23; compare Fig. 4E and Fig. 5A). At 22°C , both sigmoidicity and saturation were lost, although CGP37157 still produced a large inhibition of mitochondrial exit (Fig. 6F).

Changes in mitochondrial NADH fluorescence upon stimulation with high K^+

Several mitochondrial NADH dehydrogenases are activated by Ca^{2+} in the micromolar range (19). To check whether the increase in $[Ca^{2+}]_M$ we observed is sufficient to produce this effect, we measured endogenous NAD(P)H fluorescence (37) in chromaffin cells stimulated with high K^+ solution. In these experiments, pyruvate (2 mM) was added to the incubation solution in order to keep cytosolic NADH oxidized throughout the reaction catalyzed by lactate dehydrogenase. At the end of the experiment, the cells were perfused with 2 mM NaCN to obtain full reduction of the mitochondrial NADH by blocking electron transfer to oxygen. Figure 7 summarizes the results. Images taken at representative times during the experiment and the average trace ($\pm\text{SE}$) of 10 single cells are shown. Stimulation with high K^+ increased the NADH fluorescence by $\sim 40\%$, and this increase declined slowly after removal of the stimulus. The treatment with CN^- increased the NAD(P)H fluorescence by 100%; this increase reverted quickly upon removal of the poison.

Modeling redistribution of Ca^{2+} among different cell compartments after stimulation of chromaffin cells

Figure 8A compares fluxes (in $\mu\text{mol/l cells/s}$) estimated for entry through VOCC, mitochondrial uptake through the Ca^{2+} uniporter, and pumping by the

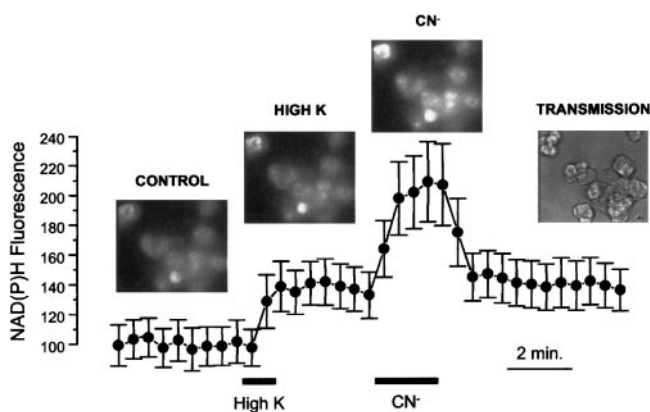


Figure 7. Effect of depolarization with high K^+ (70 mM) on mitochondrial NAD(P)H fluorescence. Temperature, 20°C . Values are the mean \pm SE of 14 single cells. CN^- , 2 mM NaCN.

plasma membrane and the SERCA ATPases at different $[Ca^{2+}]_c$. It is clear that Ca^{2+} entry overwhelms the pumps and $[Ca^{2+}]_c$ must rise quickly. Above $1 \mu\text{M}$, the mitochondrial uniporter begins to dominate Ca^{2+} transport and at $\sim 10 \mu\text{M}$ it becomes equal to Ca^{2+} entry through VOCC. Therefore, a steady state with no further change in $[Ca^{2+}]_c$ would be predicted at this concentration. We measured, however, smaller $[Ca^{2+}]_c$ concentrations during stimulation (Fig. 1). The maximal rate of mitochondrial uptake measured ($56 \mu\text{M/s} = 3300 \mu\text{mol/l cells/s}$ into one-half of the mitochondrial pool) requires $[Ca^{2+}]_c$ values of $20\text{--}40 \mu\text{M}$ (Fig. 8A; see also ref 23). On the other hand, we identify a second mitochondrial pool grouping the remaining 50% of mitochondria that takes up Ca^{2+} at rates corresponding to $[Ca^{2+}]_c$ concentrations of only $3\text{--}4 \mu\text{M}$ (23). The simplest explanation for these results is that $[Ca^{2+}]_c$ is not homogeneous but that cytosolic domains with different Ca^{2+} concentrations are established. Entry through VOCC amounts to only $\sim 10\%$ of the V_{\max} estimated for the mitochondrial uniporter (Fig. 8A). This means that as little as 10% of the mitochondria would be able to take up all the Ca^{2+} load entering through VOCC provided a near-saturating $[Ca^{2+}]_c$ is reached at the cytosolic face of this mitochondrial pool. This would slow the progress of the Ca^{2+} wave toward the core of the cell.

Figure 8B shows the predictions of a simplified model (in the upper part) that includes the transport parameters proposed here for the organelle when Ca^{2+} entry is sustained for a few seconds. The $[Ca^{2+}]_c$ concentrations graded from the subplasmalemmal region to the core of the cell within a range of more than one order of magnitude (from 0.3 to $20 \mu\text{M}$). This was because most of the Ca^{2+} load was taken up into the mitochondria physically closer to the plasma membrane. Figure 8C shows individual flows among the different compartments. After stimulation, it can be seen that uptake through the mitochondrial uniporter quickly becomes dominant and matches plasma membrane entry.

By the end of the stimulation period, $[Ca^{2+}]_c$ decreases quickly to the submicromolar range (Fig. 8B). This is because Ca^{2+} clearance from the cytosol, mainly by mitochondria, is no longer counteracted by influx through the plasma membrane. Once $[Ca^{2+}]_c$ drops below $1 \mu\text{M}$, extrusion by the plasma membrane and ER Ca^{2+} ATPases become the dominant flows and release from mitochondria through the exchanger becomes larger than uptake through the uniporter (Fig. 8C). The decrease in $[Ca^{2+}]_c$ then becomes much slower because extrusion from the cytosol is almost matched by mitochondrial release. During this period, $[Ca^{2+}]_c$ concentrations are graded from the cell core to the subplasmalemmal region (Fig. 8B) because plasma membrane extrusion takes place from this last area and Ca^{2+} released from mitochondria must diffuse toward there before being cleared.

ER plays a relatively modest role in this model. It takes up a minor fraction of Ca^{2+} during stimulation, thus contributing to sharpen the $[Ca^{2+}]_c$ domains,

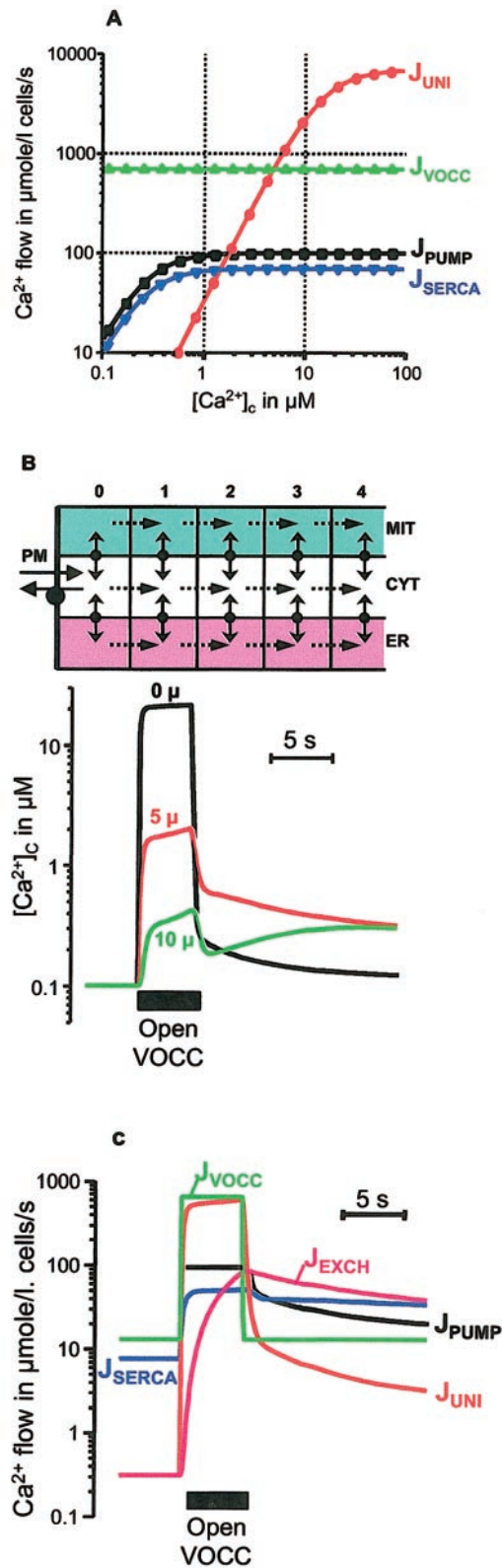


Figure 8. Predictions of a model for Ca^{2+} redistribution in chromaffin cells. *A*) Concentration dependence of the different transport systems. Flows were calculated using the equation $v = \{V_{\max} * ([\text{Ca}^{2+}]_c)^2 / \{ (K_{50})^2 + ([\text{Ca}^{2+}]_c)^2 \}$; values for V_{\max} and K_{50} for plasma membrane extrusion (J_{PUMP}), SERCA ATPase (J_{SERCA}), and mitochondrial uniporter were 100, 70, and 7000 $\mu\text{mol/l cells/s}$ and 0.25, 0.25, and 15 μM , respectively. Entry through VOCC was fixed at 700 $\mu\text{mol/l cells/s}$. *B*) Predictions of

especially at the lower $[\text{Ca}^{2+}]_c$ regions (cell core). After stimulation, ER continues accumulating Ca^{2+} as long as $[\text{Ca}^{2+}]_c$ is kept high by mitochondrial release. At longer periods (not shown), ER slowly releases its Ca^{2+} load. To keep it simpler, we have not included CICR in modeling results of Fig. 8 even though we have been able to document experimentally its operation in bovine chromaffin cells (15). When included, CICR sharpened the $[\text{Ca}^{2+}]_c$ domains observed during stimulation, as release happened preferentially from ER areas close to the plasma membrane while ER from the core was taking up Ca^{2+} from the surrounding cytosol. This Ca^{2+} diffused throughout the ER matrix to be released again near the plasma membrane.

Table 1 summarizes the main phases that can be defined from this model regarding typical $[\text{Ca}^{2+}]_c$ values and fluxes at cell, mitochondria and ER membranes (see below).

DISCUSSION

We have attempted a comprehensive quantitative explanation of fluxes taking place among the extracellular, cytosolic, and organellar compartments upon stimulation of chromaffin cells leading to Ca^{2+} entry through VOCC. Our rationale applies to entry sustained for periods of at least 1 s. It has been shown before that for stimuli lasting for milliseconds, a quite different description applies, one dominated by diffusion of Ca^{2+} through the cytosol and binding to endogenous Ca^{2+} buffers (2, 10). The smaller $[\text{Ca}^{2+}]_c$ ranges reached and the spatiotemporal restrictions may preclude a major contribution of organellar transport to shaping of the $[\text{Ca}^{2+}]_c$ peaks under this approximation. Our data, on the contrary, stress the role of organellar transport in the clearance of cytosolic Ca^{2+} . It is unclear which type of stimulus should be considered closer to physiological. Short entry would simulate better low frequency-action potentials whereas sustained entry may be closer to bursts of action potentials,

$[\text{Ca}^{2+}]_c$ at different distances from the VOCCs (0, 5, and 10 μm , as shown) during a 5 s opening of VOCCs. Ca^{2+} was assumed to enter through the plasma membrane and diffuse through 20 successive 0.5 μm cells, where it could be transported through the different transport systems with properties as in panel A. See diagram in the upper part of the panel (only the first four diffusion cells shown). Mitochondrial exit through the exchanger was modeled as $v = \{V_{\max} * ([\text{Ca}^{2+}]_M)^2 / \{ (K_{50})^2 + ([\text{Ca}^{2+}]_M)^2 \}$ where $V_{\max} = 700 \mu\text{mol/l cells/s}$ and $K_{50} = 150 \mu\text{M}$; diffusion between contiguous cells was programmed using the following first-order rate constants (s^{-1}): 50, 25, and 5 for cytosol, ER, and mitochondria, respectively. The relative volumes and Ca^{2+} activity coefficients for cytosol, ER, and mitochondria were 0.85, 0.10, and 0.05 and 1/40, 1/20, and 1/1000, respectively. $[\text{Ca}^{2+}]_c$ and $[\text{Ca}^{2+}]_{\text{ER}}$ at rest were assumed to be 0.1 and 610 μM , respectively; first-order leaks through the plasma membrane and the ER membrane were programmed accordingly. *C*) Ca^{2+} flows through the different transport systems during a 5 s opening of VOCCs. Details as in panel B.

TABLE 1. *Different phases of cell Ca^{2+} homeostasis after stimulation of Ca^{2+} entry through VOCC*

Phase	$[\text{Ca}^{2+}]_c$	Fluxes
0 (Prestimulus)	Resting	All fluxes at steady state
S (Stimulus)	$>1 \mu\text{M}$ Graded from PM to core	PM: influx \gg efflux MIT: uptake \gg release PM influx \cong MIT uptake ER: uptake $>$ release or vice versa ^a
PS1 (Early poststimulus)	Quick decrease to $<1 \mu\text{M}$	PM: efflux $>$ influx MIT: uptake $>$ release $-d[\text{Ca}^{2+}]_c \cong$ MIT uptake ER: uptake $>$ release
PS2 (Late poststimulus)	$<1 \mu\text{M}$; Slow decrease to resting Graded from core to PM	PM: efflux $>$ influx MIT: release $>$ uptake ER: first uptake $>$ release, then vice versa
0	Resting	All fluxes at steady state

^a Depends on the activity of ryanodine receptors. PM: plasma membrane; MIT: mitochondria; ER: endoplasmic reticulum.

as is the case at the splanchnic nerve–chromaffin cell synapse (38), or to maintained action of acetylcholine or other chemical stimuli.

We find several new properties of mitochondrial Ca^{2+} transport systems acting on intact cells using targeted low Ca^{2+} affinity aequorins, which are able to measure near millimolar $[\text{Ca}^{2+}]_M$. For example, maximum capacity of the mitochondrial uniporter approaches 6000–7000 $\mu\text{mol}/1 \text{ cells}/\text{s}$, a value well above most previous proposals. Previous estimates of Ca^{2+} accumulation by mitochondria of rat chromaffin cells (13) or frog sympathetic neurons (35, 39, 40) are in the range of 50–200 $\mu\text{mol}/1 \text{ cells}/\text{s}$ at $[\text{Ca}^{2+}]_c$ concentrations of 0.5–2 μM . However, the uniporter shows second-order kinetics with regard to Ca^{2+} (18); since these concentrations are well below saturation of the transport system ($K_{50}=10\text{--}40 \mu\text{M}$), it is not possible to extrapolate reliable V_{max} values from these data. Increasing $[\text{Ca}^{2+}]_c$ over a much wider range ($\leq 200 \mu\text{M}$) by photon-induced Ca^{2+} release from DM-dinitrophen, Xu et al. (6) estimated in bovine chromaffin cells V_{max} values of 4800 $\mu\text{mol}/1 \text{ cells}/\text{s}$, a value close to the one reported here. Dialysis of cytosolic components in cells maintained under whole cell patch, which decreases \sim eightfold the activity of the uniporter (21), could also contribute to explain differences with previous results. Therefore, we believe that the high rates of uptake reported here are representative of the real values in intact cells. This implies that mitochondria can take up most of the Ca^{2+} load entering the cells through VOCC if cytosolic Ca^{2+} concentrations high enough to activate the uniporter are built up. The idea that mitochondria can contribute to clearing Ca^{2+} loads from the cytosol has already been proposed for chromaffin cells (6, 21, 23) and pancreatic acinar cells (41, 42), but we provide a solid quantitative argument.

Our model predicts that a fraction of the mitochondrial pool closer to the plasma membrane can sink most of the Ca^{2+} load entering through VOCC during several seconds (Fig. 8). This results in the generation

of subcellular domains with different $[\text{Ca}^{2+}]_c$. Thus, high Ca^{2+} domains are restricted to the subplasmalemmal region, whereas low Ca^{2+} domains locate at the core of the cell. Mitochondria act as biosensors to discriminate high and low Ca^{2+} domains. Second-order kinetics of the uptake through the uniporter sharpens differences in $[\text{Ca}^{2+}]_c$ above and below a threshold located near its K_{50} , 10^{-5} M . Taking advantage of the fact that the native, high Ca^{2+} affinity aequorin is fully burned up within a few seconds into a high Ca^{2+} ($>10^{-5} \text{ M}$) environment, we have defined two mitochondrial pools, M1 and M2, each amounting to $\sim 50\%$ of the total, which differ by their rate of Ca^{2+} uptake after cell stimulation (23). Pool M1 takes up Ca^{2+} at rates of $> 50 \mu\text{M}/\text{s}$ (Fig. 5) corresponding to $[\text{Ca}^{2+}]_c$ concentrations of $> 20 \mu\text{M}$ (Fig. 8A). Pool M2 takes up Ca^{2+} at only $0.3 \mu\text{M}/\text{s}$, corresponding to 2–3 μM $[\text{Ca}^{2+}]_c$ (23). Electron microscopy X-ray microanalysis of frog sympathetic neurons after stimulation with high K^+ also revealed the existence of two mitochondrial pools with different Ca^{2+} contents (35). In pancreatic acinar cells, entry of Ca^{2+} through plasma membrane also caused preferential Ca^{2+} uptake into subplasmalemmal mitochondria (42).

Continuity of the intramitochondrial space seems much greater than previously thought (43, 44). Thus, it is conceivable that the Ca^{2+} load that fills the M1 pool may have been taken up by a smaller fraction of mitochondria close to the plasma membrane Ca^{2+} channels, then diffused throughout the mitochondrial matrix to invade a larger fraction of the mitochondrial pool. According to the figures used here for V_{max} of the uniporter and Ca^{2+} entry through VOCC, the full Ca^{2+} load could be taken up by only 10% of the mitochondrial pool if a high enough $[\text{Ca}^{2+}]_c$ is reached. Assuming a spherical shape for the cells and uniform distribution of mitochondria, 10% of the mitochondrial space would occupy only $0.25 \mu\text{m}$ beneath the plasma membrane in a $15 \mu\text{m}$ diameter cell.

Neher and co-workers first elaborated the idea that

transient opening of VOCC during action potentials should generate high Ca^{2+} microdomains near the channel mouth. Such microdomains are highly restricted in time (ms scale) and space (nm scale) due to dissipation by rapid diffusion of Ca^{2+} to the surrounding cytosol. The existence of such microdomains as well as the constrictions imposed by diffusion and binding to cytosolic Ca^{2+} buffers has been convincingly documented in bovine chromaffin cells (2, 10). The high Ca^{2+} subcellular domains proposed here are maintained for seconds because of the pump/leak steady state established between Ca^{2+} entry and mitochondrial uptake. We have no indication of the size of such domains, although they would probably be bigger than microdomains. When modeling, the ratio between the V_{max} of the uniporter and the diffusion coefficient is important in determining the shape of the $[\text{Ca}^{2+}]_c$ gradation, which becomes sharper the larger this ratio is. For these reasons, the present model should be regarded as a crude approximation. For example, denser packing of the organella or slower diffusion rates at the subplasmalemmal region would render gradation of Ca^{2+} domains steeper. Previous observations on irregular progression of the Ca^{2+} wave at this region (7) suggest that such physical constraints may apply.

After stimulation, two phases can be defined in the relaxation of the $[\text{Ca}^{2+}]_c$ peak (Table 1). In the early poststimulation period (PS1), $[\text{Ca}^{2+}]_c$ drops quickly to concentrations below 1 μM mainly because of rapid clearance from the cytosol by mitochondrial uptake. After this initial drop, $[\text{Ca}^{2+}]_c$ decreases much more slowly, as extrusion through the plasma membrane is counteracted by mitochondrial Ca^{2+} release (late poststimulation period; PS2 in Table 1). This phase is usually evident in fura-2 measurements as a long period when $[\text{Ca}^{2+}]_c$ remains moderately increased above resting levels. It has been reported that collapsing the mitochondrial membrane potential by addition of protonophores induces a $[\text{Ca}^{2+}]_c$ increase by mitochondrial Ca^{2+} release, but only for a short period after the end of stimulation (13, 21). We have documented recently that protonophores may induce rapid release of mitochondrial Ca^{2+} by reversal of the Ca^{2+} uniporter, but this requires relatively high $[\text{Ca}^{2+}]_c$ (24), a condition accomplished only during period PS1. During the PS2 period, $[\text{Ca}^{2+}]_c$ is graded from the cell core to the subplasmalemmal region. In the last region $[\text{Ca}^{2+}]_c$ drops very quickly to the resting level, thus securing the end of exocytosis, by action of the plasma membrane Ca^{2+} extrusion mechanisms. At the cell core, $[\text{Ca}^{2+}]_c$ remains discretely high for many seconds because of the relatively slow release of the mitochondrial load. Perhaps this maintained increase helps mobilize new secretory vesicles from the reserve pool toward the plasma membrane, thus becoming ready to be used for the next exocytotic episode (2).

Exit of the Ca^{2+} load from mitochondria occurs primarily through the $\text{Na}^+/\text{Ca}^{2+}$ exchanger (Fig. 6; ref

19). We also document some new properties for the in situ operation of this transport system. First, activity is much faster than most of previous estimates in isolated mitochondria (18, 19). The same reasons cited above for the uniporter may apply here. Moreover, the mitochondrial $\text{Na}^+/\text{Ca}^{2+}$ exchanger is very sensitive to temperature (Fig. 6), which was 20°C in most of the previous estimates. Another new finding was the sigmoidal, second-order kinetics of $[\text{Ca}^{2+}]_M$. The activity of this transport system had been reported to show Michaelian first-order kinetics with regard to Ca^{2+} in experiments with isolated mitochondria (18). Again, temperature may explain some of the discrepancies, as sigmoidicity disappears at 20°C (Fig. 6). Sigmoidicity also disappeared in the presence of the inhibitor CGP37157 (Fig. 6), thus excluding an artifact generated by the measuring procedure.

Second-order kinetics fits well with the high rates of mitochondrial Ca^{2+} clearance observed at high $[\text{Ca}^{2+}]_M$ and the rapid decline when $[\text{Ca}^{2+}]_M$ decreases (Fig. 6). Accordingly, $[\text{Ca}^{2+}]_M$ would remain in the micromolar range several minutes after the stimulus. Stimulation of pyruvate- and α -ketoglutarate-dehydrogenase by Ca^{2+} has been reported to be complete at $> 3 \mu\text{M}$ (16, 19). Thus, residual Ca^{2+} would keep these dehydrogenases active during the poststimulus period, as suggested by NAD(P)H fluorescence measurements (Fig. 7). The stimulation of respiration may help to provide energy for clearing the Ca^{2+} load. Isocitrate dehydrogenase shows stimulation by Ca^{2+} at higher concentration ranges (2×10^{-5} to 1×10^{-4} M; ref 19) so that activity of this enzyme may change during period PS1.

In summary, our results suggest a highly structured spatiotemporal organization of Ca^{2+} signals originated by sustained Ca^{2+} entry through VOCC in adrenal chromaffin cells. High $[\text{Ca}^{2+}]_c$ domains suitable for triggering exocytosis are generated at the subplasmalemmal region. Domains with a smaller $[\text{Ca}^{2+}]_c$ increase but more sustained in time (adequate for mobilizing the reserve pool of secretory vesicles; ref 2) are generated at the core regions of the cytosol and at the nucleus. Mitochondria seem to be essential for shaping these local Ca^{2+} domains. On the other hand, Ca^{2+} uptake by mitochondria activates NADH-dehydrogenases, thus tuning up respiration to match the increased local energy needs (16). Full relaxation of the $[\text{Ca}^{2+}]_c$ peak requires clearance of the mitochondrial Ca^{2+} load through the $\text{Na}^+/\text{Ca}^{2+}$ exchanger, which proceeds slowly at low micromolar $[\text{Ca}^{2+}]_M$ levels. This keeps respiration stimulated and core $[\text{Ca}^{2+}]_c$ discretely high for a long period after stimulation, acting as a kind of memory that may help to secure restoration of the initial conditions. **[FJ]**

This work was supported by the Spanish Dirección General de Enseñanza Superior (DGES, grants PB97-0474, APC1999-011, and 1FD97-1725-C02-02 to J.G.S., PM98-0142 to J.A., and PM99-0005 to A.G.G.) and the Instituto de Salud Carlos III (to A.G.G.). C.V. and L.N. hold postdoctoral fellowships from the Spanish DGES.

REFERENCES

- Douglas, W. W. (1968) Stimulus-secretion coupling: the concept and clues from chromaffin and other cells. *Br. J. Pharmacol.* **34**, 453–474
- Neher, E. (1998) Vesicle pools and Ca^{2+} microdomains: new tools for understanding their roles in neurotransmitter release. *Neuron* **20**, 389–399
- Alvarez, J., Montero, M., and García-Sancho, J. (1999) Subcellular Ca^{2+} dynamics. *Neurosci. Biophys. Sci.* **14**, 161–168
- Berridge, M. J., Lipp, P., and Bootman, M. D. (2000) The versatility and universality of calcium signalling. *Nat. Rev. Mol. Cell. Biol.* **1**, 11–21
- Zhou, Z., and Neher, E. (1993) Mobile and immobile calcium buffers in bovine adrenal chromaffin cells. *J. Physiol. (London)* **469**, 245–273
- Xu, T., Naraghi, M., Kang, H., and Neher, E. (1997) Kinetic studies of Ca^{2+} binding and Ca^{2+} clearance in the cytosol of adrenal chromaffin cells. *Biophys. J.* **73**, 53
- Naraghi, M., Müller, T. H., and Neher, E. (1998) Two-dimensional determination of the cellular Ca^{2+} binding in bovine chromaffin cells. *Biophys. J.* **75**, 1635–1647
- Neher, E., and Augustine, G. J. (1992) Calcium gradients and buffers in bovine chromaffin cells. *J. Physiol. (London)* **450**, 273–301
- Augustine, G. J., and Neher, E. (1992) Calcium requirements for secretion in bovine chromaffin cells. *J. Physiol. (London)* **450**, 247–271
- Neher, E. (1998) Usefulness and limitations of linear approximations to the understanding of Ca^{2+} signals. *Cell Calcium* **24**, 345–357
- Petersen, O. H. (1996) Can Ca^{2+} be released from secretory granules or synaptic vesicles? *Trends Neurosci.* **19**, 411–413
- Park, Y. B., Herrington, J., Babcock, D. F., and Hille, B. (1996) Ca^{2+} clearance mechanisms in isolated rat adrenal chromaffin cells. *J. Physiol. (London)* **492**, 329–346
- Herrington, J., Park, Y. B., Babcock, D. F., and Hille, B. (1996) Dominant role of mitochondria in clearance of large Ca^{2+} loads from rat adrenal chromaffin cells. *Neuron* **16**, 219–228
- Artalejo, C. R., García, A. G., and Aunis, D. (1987) Chromaffin cell calcium kinetics measured isotopically through fast calcium, strontium, and barium fluxes. *J. Biol. Chem.* **262**, 915–926
- Alonso, M. T., Barrero, M. J., Michelena, P., Carnicero, E., Cuchillo, I., García, A. G., García-Sancho, J., Montero, M., and Alvarez, J. (1999) Ca^{2+} -induced Ca^{2+} release in chromaffin cells seen from inside the ER with targeted aequorin. *J. Cell Biol.* **144**, 241–254
- Rizzuto, R., Bernardi, P., and Pozzan, T. (2000) Mitochondria as all-round players of the calcium game. *J. Physiol. (London)* **529**, 37–47
- Duchen, M. R. (2000) Mitochondria and calcium: from cell signalling to cell death. *J. Physiol. (London)* **529**, 57–68
- Gunter, T. E., and Pfeiffer, D. R. (1990) Mechanisms by which mitochondria transport calcium. *Am. J. Physiol.* **258**, C755–C786
- Gunter, T. E., Gunter, K. K., Sheu, S. S., and Gavin, C. E. (1994) Mitochondrial calcium transport: physiological and pathological relevance. *Am. J. Physiol.* **267**, C313–C339
- Coll, K. E., Joseph, S. K., Corkey, B. E., and Williamson, J. R. (1982) Determination of the matrix free Ca^{2+} concentration and kinetics of Ca^{2+} efflux in liver and heart mitochondria. *J. Biol. Chem.* **257**, 8696–8704
- Babcock, D. F., Herrington, J., Goodwin, P. C., Park, Y. B., and Hille, B. (1997) Mitochondrial participation in the intracellular Ca^{2+} network. *J. Cell Biol.* **136**, 833–844
- Horikawa, Y., Goel, A., Somlyo, A. P., and Somlyo, A. V. (1998) Mitochondrial calcium in relaxed and tetanized myocardium. *Biophys. J.* **74**, 1579–1590
- Montero, M., Alonso, M. T., Carnicero, E., Cuchillo-Ibanez, I., Albillos, A., García, A. G., García-Sancho, J., and Alvarez, J. (2000) Chromaffin-cell stimulation triggers fast millimolar mitochondrial Ca^{2+} transients that modulate secretion. *Nat. Cell Biol.* **2**, 57–61
- Montero, M., Alonso, M. T., Albillos, A., García-Sancho, J., and Alvarez, J. (2001) Mitochondrial Ca^{2+} -induced Ca^{2+} release mediated by the Ca^{2+} uniporter. *Mol. Biol. Cell* **12**, 63–71
- Alonso, M. T., Barrero, M. J., Carnicero, E., Montero, M., García-Sancho, J., and Alvarez, J. (1998) Functional measurements of $[\text{Ca}^{2+}]$ in the endoplasmic reticulum using a herpes virus to deliver targeted aequorin. *Cell Calcium* **24**, 87–96
- Nuñez, L., De La Fuente, M. T., García, A. G., and García-Sancho, J. (1995) Differential Ca^{2+} responses of adrenergic and noradrenergic chromaffin cells to various secretagogues. *Am. J. Physiol.* **269**, C1540–C1546
- Chiesa, A., Rapizzi, E., Tosello, V., Pinton, P., De Virgilio, M., Fogarty, E., and Rizzuto, R. (2001) Recombinant aequorin and green fluorescent protein as valuable tools in the study of cell signalling. *Biochem. J.* **355**, 1–12
- Montero, M., Brini, M., Marsault, R., Alvarez, J., Sitia, R., Pozzan, T., and Rizzuto, R. (1995) Monitoring dynamic changes in free Ca^{2+} concentration in the endoplasmic reticulum of intact cells. *EMBO J.* **14**, 5467–5475
- Montero, M., Barrero, M. J., and Alvarez, J. (1997) $[\text{Ca}^{2+}]$ microdomains control agonist-induced Ca^{2+} release in intact HeLa cells. *FASEB J.* **11**, 881–885
- Alvarez, J., and Montero, M. (2001) Ca^{2+} measurement with luminescent probes in the endoplasmic reticulum. In *Measuring Calcium and Calmodulin Inside and Outside Cells* (Petersen, O. H., ed) pp. 147–163, Springer Lab Manual, Springer, Berlin
- Frawley, L. S., Faught, W. J., Nicholson, J., and Moomaw, B. (1994) Real time measurement of gene expression in living endocrine cells. *Endocrinology* **135**, 468–471
- Rutter, G. A., Burnett, P., Rizzuto, R., Brini, M., Murgia, M., Pozzan, T., Tavares, J. M., and Denton, R. M. (1996) Subcellular imaging of intramitochondrial Ca^{2+} with recombinant targeted aequorin: significance for the regulation of pyruvate dehydrogenase activity. *Proc. Natl. Acad. Sci. USA* **93**, 5489–5494
- Barrero, M. J., Montero, M., and Alvarez, J. (1997) Dynamics of $[\text{Ca}^{2+}]$ in the endoplasmic reticulum and cytoplasm of intact HeLa cells. A comparative study. *J. Biol. Chem.* **272**, 27694–27699
- Mogami, H., Gardner, J., Gerasimenko, O. V., Camello, P., Petersen, O. H., and Tepikin, A. V. (1999) Calcium binding capacity of the cytosol and endoplasmic reticulum of mouse pancreatic acinar cells. *J. Physiol. (London)* **518**, 463–467
- Pivovarova, N. B., Hongpaisan, J., Andrews, S. B., and Friel, D. D. (1999) Depolarization-induced mitochondrial Ca accumulation in sympathetic neurons: spatial and temporal characteristics. *J. Neurosci.* **19**, 6372–6384
- Uceda, G., García, A. G., Guantes, J. M., Michelena, P., and Montiel, C. (1995) Effects of Ca^{2+} channel antagonist subtypes on mitochondrial transport. *Eur. J. Pharmacol.* **289**, 73–80
- Hajnoczky, G., Robb-Gaspers, L. D., Seitz, M. B., and Thomas, A. P. (1995) Decoding of cytosolic calcium oscillations in the mitochondria. *Cell* **82**, 415–424
- Holman, M. E., Coleman, H. A., Tonta, M. A., and Parkinson, H. C. (1994) Synaptic transmission from splanchnic nerves to the adrenal medulla of guinea-pigs. *J. Physiol. (London)* **478**, 115–124
- Friel, D. D., and Tsien, R. W. (1994) An FCCP-sensitive Ca^{2+} store in bullfrog sympathetic neurons and its participation in stimulus-evoked changes in $[\text{Ca}^{2+}]$. *J. Neurosci.* **14**, 4007–4024
- Colegrove, S. L., Albrecht, M. A., and Friel, D. D. (2000) Dissection of mitochondrial Ca^{2+} uptake and release fluxes in situ after depolarization-evoked $[\text{Ca}^{2+}]$ elevations in sympathetic neurons. *J. Gen. Physiol.* **115**, 351–370
- Tinel, H., Cancela, J. M., Mogami, H., Gerasimenko, J. V., Gerasimenko, O. V., Tepikin, A. V., and Petersen, O. H. (1999) Active mitochondria surrounding the pancreatic acinar granule region prevent spreading of inositol trisphosphate-evoked local cytosolic Ca^{2+} signals. *EMBO J.* **18**, 4999–5008
- Park, M. K., Ashby, M. C., Erdemli, G., Petersen, O. H., and Tepikin, A. V. (2001) Perinuclear, perigranular and sub-plasmalemmal mitochondria have distinct functions in the regulation of cellular calcium transport. *EMBO J.* **20**, 1863–1874
- Rizzuto, R., Pinton, P., Carrington, W., Fay, F. S., Fogarty, K. E., Lifshitz, L. M., Tuft, R. A., and Pozzan, T. (1998) Close contacts with the endoplasmic reticulum as determinants of mitochondrial Ca^{2+} responses. *Science* **280**, 1763–1766
- Skulachev, V. P. (2001) Mitochondrial filaments and clusters as intracellular power-transmitting cables. *Trends Biochem. Sci.* **26**, 23–29

Received for publication September 28, 2001.

Accepted for publication November 6, 2001.